

# Real-Time Prediction of Lower Limb Joint Kinematics, Kinetics, and Ground Reaction Force using Wearable Sensors and Machine Learning

Josée Mallah, Yu Zhu, Kailang Xu, Gurvinder S. Virk, *Senior Member, IEEE*, Shaoping Bai, *Senior Member, IEEE*, and Luigi G. Occhipinti\*, *Senior Member, IEEE*

**Abstract— Objective:** Walking is a key movement of interest in biomechanics, yet gold-standard data collection methods are time- and cost-expensive. This paper presents a real-time, multimodal, high sample rate lower-limb motion capture framework, based on wireless wearable sensors and machine learning algorithms. **Methods:** Random Forests are used to estimate joint angles from IMU data, and ground reaction force (GRF) is predicted from instrumented insoles, while joint moments are predicted from angles and GRF using deep learning based on the ResNet-16 architecture. **Results:** All three models achieve good accuracy compared to literature, and the predictions are logged at 1 kHz with a minimal delay of 23 ms for 20s worth of input data. **Conclusion:** We were able to achieve decently accurate predictions with minimal delay. **Significance:** The present work fully relies on wearable sensors, covers all five major lower limb joints, and provides multimodal comprehensive estimations of GRF, joint angles, and moments with minimal delay suitable for biofeedback applications.

**Index Terms**—wearable sensors, machine learning, biomechanics, real-time systems

## I. INTRODUCTION

WALKING is a basic locomotion skill and consists in most of human daily movement; it involves interaction of bony alignment, joint range of motion, neuromuscular activity, and the physics rules of motion, which makes it a relevant activity to be studied in the field of biomechanics, with gait analysis specializing in the assessment of gait and detection of abnormalities [1]. Joint angles and moments and ground reaction force are key variables in gait analysis. Joint angles describe the orientation of two articulated segments at a joint

This work was supported by the MathWorks-CUED Small Grant Programme 2024 and 2025. J. Mallah is supported by the Cambridge Trust via an Allen, Meek, and Read Cambridge International Scholarship. L. G. Occhipinti acknowledges funding from UK Research Council (EPSRC (grants EP/W024284/1, EP/P027628/1) and from the British Council (UKIERI Contract No. 45371261).

J. Mallah, Yu Zhu, Kailang Xu, and Luigi G. Occhipinti\* are with the Electrical Engineering Division, Department of Engineering, University of Cambridge, Cambridge CB3 0FA, United Kingdom (correspondence e-mail: [lgo23@cam.ac.uk](mailto:lgo23@cam.ac.uk)). Yu Zhu is with the Department of Electronic Systems, Aalborg University, Aalborg 9220, Denmark. Gurvinder Virk is with

and are clinically used to assess joint function as part of gait analysis procedures [2]. Joint moments describe the forces acting on joints and are used in the evaluation of motor function [3], [4], [5], [6], [7] as well as in the design and control of assistive devices such as prostheses [8], [9] and exoskeletons [10], [11], [12], [13]. GRF is important in evaluating ground contact, and is often used along with joint angles to compute joint moments [14].

The traditional golden standard procedure to measure joint angles during motion is to use an optical motion capture system based on cameras and markers placed on the human body to record the movement and then perform an inverse kinematics analysis on the marker trajectories to extract the angles. On the other hand, GRF measurement is generally based on force plates and instrumented treadmills. Joint moments are then calculated using an inverse dynamics analysis from the kinematics results along with the GRF data. Both inverse kinematics and inverse dynamics are performed offline after data collection in a musculoskeletal simulation software such as OpenSim [14] and Anybody [15]. However, optical motion capture systems and force plates are expensive and require a suitable lab space to be installed in, the measurement is limited by the number of available force plates [16], [17], which also impacts the motion of the subject [18], [19], and marker placement as well as the data processing procedures are time-consuming and often requiring manual setup and specific technical skills [20], meaning that this procedure cannot be deployed in real time outside the lab, such as in everyday environments or within wearable assistive devices [1]. While markerless motion capture has recently been proposed as a more portable, less skill- and time-consuming solution [20], [21], commercial systems are still relatively expensive and require the use of powerful computers [22].

Endoenergy Systems Ltd., Cambridge, United Kingdom, and with Huzhou Wuxing District Intelligent Robot Innovation Research Institute, China. Shaoping Bai is with the Department of Materials and Production, Aalborg University, Aalborg 9220, Denmark.

All experimental procedures involving human subjects were approved by the Department of Engineering Ethics Committee at the University of Cambridge (Reference No. 639). The study was conducted in accordance with institutional guidelines and the Declaration of Helsinki.

Supplementary material, consisting mostly of additional figures and tables, are available online.

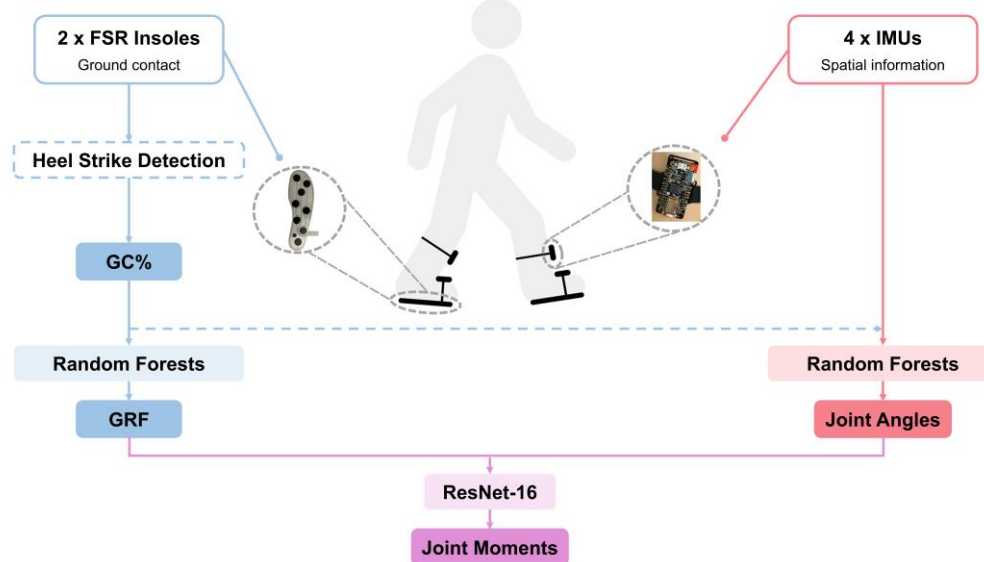


**Fig. 1.** In this paper, Random Forests are used to estimate joint angles from IMU data, and GRF from instrumented insoles, while joint moments are predicted from angles and GRF using deep learning using a model based on the ResNet-16 architecture.

For purposes of joint angle tracking, inertial measurement units (IMUs) are seen as a low-cost alternative for real-time deployment, able to provide segment orientation estimates by integrating linear acceleration, angular velocity, and magnetometer data and using sensor-fusion algorithms such as Kalman filters, complementary filters, and gradient descent algorithms [2], [23], [24]. This process faces several challenges, including sensor drift and difficulties aligning the sensors to body segments and anatomical references [2], [23], [25], but machine learning algorithms can be used [2], [23], [26], [27], [28] and seem to overcome these challenges. Similarly, sensor-instrumented insoles have recently been proposed, in particular those embedded with force sensitive resistors (FSRs) [29], [30], [31], [32], and were shown to be a good wearable alternative to force plates, being unobtrusive, inexpensive, and having a low power consumption, while not affecting gait patterns [2].

This paper presents a real-time, multimodal, high sample rate lower-limb motion capture framework (Fig. 1). The Random Forests algorithm is used to predict ankle angles using IMUs placed on the shank and foot, as well as to predict the vertical ground reaction force (vGRF) from flexible wearable insoles embedded with force myography (FMG) sensors. Weight-normalized vGRF is then added to the feature set of the angle prediction model, allowing for better predictions. Deep learning models based on the ResNet-16 architecture are then used as a replacement for inverse dynamics analyses to estimate ankle joint moments from the ankle angle and vertical GRF. The study is then extended to predict 5 lower limb joint angles and moments – hip flexion, adduction, and rotation, knee flexion, and ankle flexion.

## II. METHODS

### A. Data Collection

8 young healthy subjects were recruited for the experiment (3 females and 5 males, age:  $24.5 \pm 3.1$  years, height:  $177.1 \pm 9.7$  cm, weight:  $72.7 \pm 12.9$  kg). Motion capture data was collected

using 16 Vicon Valkyrie VK26 cameras (©Vicon Motion Systems Ltd., Oxford, UK), 41 reflective markers (9 mm, ©B&L Engineering, California, USA), and 3 AMTI ground embedded force plates (2 of  $46 \times 51$  cm, and 1 of  $40 \times 60$  cm, ©Advanced Mechanical Technology, Inc., Watertown USA). Additionally, 4 thermal FLIR cameras (© Teledyne FLIR LLC, Oregon, USA) provided video recording. 9-axis (3D accelerometer, gyroscope, and magnetometer) commercial and open-source EmotiBit IMUs (© Connected Future Labs LLC, Nevada, USA) were worn bilaterally on the shanks and feet, and the data was collected at 25 Hz and transmitted wirelessly to a computer via UDP, but data from all 4 IMUs was only available for four subjects due to sensors disconnecting (1 female and 3 males, age:  $23.75 \pm 2.05$  years, height:  $180.75 \pm 10.96$  cm, weight:  $82.0 \pm 10.86$  kg). Five subjects (2 females and 3 males, age:  $25.2 \pm 3.43$  years, height:  $179.4 \pm 7.99$  cm, weight:  $76 \pm 11.66$  kg) wore sandals instrumented with insoles (design inspired by [2]) embedded with 8 FSR-based FMG sensors [19] each. All subjects walked in straight lines at their self-selected speeds.

### B. Data Pre-Processing

An OpenSim model is scaled to the dimensions of each subject using static trial data, and the inverse kinematics tool is executed using marker trajectories from the dynamic trials; the gait2392 model is used. The kinematics results are fed into the inverse dynamics tool along with the force plate data to compute the joint moments. Joint angles and moments are up-sampled from 100 Hz to 1 kHz. The IMU data is also up-sampled to 1 kHz using linear interpolation, and bandpass filtered using a fifth-order Butterworth filter with cut-off frequencies of 0.2 and 10 Hz. The marker and IMU data were synchronized using UNIX timestamps and trimmed to the gait cycle duration, which was delimited as follows: for each walking trial, 3 heel strikes are identified from force plate data (20 N threshold), and the fourth heel strike that marks the end

of the second stride is determined using the velocity of the heel markers. Hence gait cycle percentages (GC%) corresponding to each datapoint could be generated. The force plate and FSR data were synchronized using UNIX timestamps and trimmed to the gait cycle duration. The vertical component of the ground reaction force was considered and normalized by body weight. FSR data is lowpass filtered at 3 Hz using a fifth-order Butterworth filter. GRF data used in the angle models are normalized by body mass.

### C. Machine Learning Models

Model input data was scaled using a Standard Scaler to have zero mean and unit variance. All models were trained using two methods: (1) intra-subject, performing k-fold cross validation ( $k=5$  for GRF and angles,  $k=4$  for moments) while combining the data from all subjects, shuffling it, and splitting it by gait cycle, and (2) inter-subject, applying *LeaveOneSubjectOut* Cross Validation (LOSOCV).

#### 1) GRF Model

The Random Forest algorithm is used, for its robustness to relatively small datasets due its non-parametric learning method apart from the number of trees [2, 20, 21]. Instead of using time-series machine learning algorithms, GC% is used along with the FSR data for vGRF prediction to add a temporal dimension to the network that is independent of the walking speed, while simplifying the model independently from hyperparameter tuning and significantly reducing the risk of overfitting and training time. The model was trained using Scikit Learn default settings (100 trees).

#### 2) Angle Models

The models were also developed using the Random Forest algorithm, which is preferred over deep learning algorithms such as CNN or LSTM to reduce complexity when low latency is crucial [33], [34], [35], which makes Random Forests the best trade-off in terms of speed, accuracy, interpretability, and simplicity [26], [35], [36]. For the walking trials, and instead of using time-series machine learning algorithms, GC% is used as an input to add a temporal dimension to the network that is independent of the walking speed, and can also be obtained in real-time from insoles or heel contact sensors [37], [38], along with a Boolean flag to indicate the leading foot (on which GC% calculation is based). The main model inputs are 9 channels from each IMU. Models use inputs from either 2 IMUs from the same leg to predict the corresponding ankle angle (unilateral), or 4 IMUs from both legs to predict both ankle angles (bilateral). The study was then extended to predict 5 lower limb angles: hip flexion, adduction, and rotation, knee flexion, as well as ankle flexion. Several models were developed using different combinations of inputs and outputs as shown in Table I. Model settings were specified in Scikit Learn (200 trees, `max_depth=None`, `min_samples_split=2`, `min_samples_leaf=1`).

TABLE I  
DIFFERENT MODEL INPUT AND OUTPUT COMBINATIONS

Model Name	Inputs	Output Angles
W1	20 (2 IMUs, GC%, flag)	
W2	21 (2 IMUs, GRF, GC%, flag)	1: ankle
W3	40 (4 IMUs, 2 GRF, GC%, flag)	2: ankles (right, left)
W4	20 (2 IMUs, GC%, flag)	5: 3D hip, knee,
W5	21 (2 IMUs, GRF, GC%, flag)	ankle
W6	40 (4 IMUs, 2 GRF, GC%, flag)	10: 3D hips, knees, ankles (right, left)

#### 3) Moment Models

A deep learning model based on the ResNet-16 architecture and 1D convolutional neural networks (CNN) layers was used. This a time-series model, and similar architectures have been used for similar applications [39], [40], [41]. The model starts with an initial convolutional block including 1D convolution, batch normalization, and ReLU activation layers, to help reduce the time dimension while extracting features. 4 residual blocks follow, allowing for deep feature extraction without vanishing gradients. A global average pooling operation follows, along with a fully connected dense layer and an output layer consisting of 2 neurons, one for each output variable. The network was trained using the ADAM optimizer and mean squared error (MSE) loss over 500 epochs, while implementing early stopping with a patience of 10 epochs and restoring the best weights.

The input ankle joint angles and GRF data were scaled using a Standard Scaler to have zero mean and unit variance. Two other inputs were added: GC%, and a Boolean flag to indicate the leading foot. The input data were passed to the model in windows of 10ms.

In a second instance, we extend our model to predict the 5 main lower limb joint moments – hip flexion, adduction, and rotation, knee flexion, and ankle flexion – based on the corresponding joint angles and vertical GRF, along with GC% and the lead/lag flag. The same ResNet-16 architecture is deployed and trained using the same intra-subject and inter-subject methods.

#### 4) Performance Evaluation

vGRF and joint moment estimation performance was assessed using the mean absolute error (NMAE) and the mean root mean square error (NRMSE) both normalized by range. Additionally, the Pearson correlation coefficient ( $r$ ) and the coefficient of determination ( $r^2$ ) were computed for predictions and test data. Angle estimation performance on the test set was assessed using the mean root mean squared error (RMSE).

#### 5) Model Chaining

While joint angles and GRF data used in training and evaluating the moment prediction model were obtained using the normal procedure involving motion capture systems and musculoskeletal models, we want to test the applicability of our model to real-time walking scenarios, using data provided by wearable sensors, i.e. IMUs and FSRs. Therefore, the predictions provided by the angle and GRF models will feed

into the ankle moment prediction model.

#### 6) Real-Time System

Near real-time motion capture, including ground reaction force data as well as lower limb joint angles and moments during walking of healthy subjects is achieved using 2 IMUs and one FSR-instrumented insole per leg.

The code is developed in Python and run wirelessly on a computer 13<sup>th</sup> Gen Intel® Core™ i7-13700, 2100 MHz, 16 Cores, 24 Logical Processors. The program collects data from the sensors, and performs timestamp adjustment, up-sampling (IMU), and filtering. Heel strikes are detected from the insole data and used to calculate the gait cycle percentage needed for the predictors (from the previous stride). GRF and angle predictions are then made based on the insole and IMU data, respectively (GRF was not integrated in angle prediction: model W4), and feed into the moment predictor for estimating the joint moments. The extended angle and moment models were used, providing data for the 5 major lower limb joint angles: hip flexion, adduction, and rotation, knee flexion, and ankle flexion. The angle and moment predictions obtained are rather noisy, therefore a low pass filter was applied to clean it. All the data is saved in log files: insole raw, timestamp-adjusted, and filtered; IMU raw, up-sampled, and filtered; GRF predictions; raw and filtered angle and moment predictions.

The program was tested on a healthy subject (age: 21 years, height: 178 cm, weight: 59 kg), using a 20s trial time for data collection.

To evaluate the quality of the predictions, we calculate Pearson's  $r$  between the mean profile of the initial dataset (which was used for training and offline testing) and real-time (RT) predictions

### III. RESULTS

#### A. GRF Model

The vGRF model achieves an  $\text{NRMSE} \pm 0.61\%$  in intra-subject mode, and  $8.36 \pm 0.91\%$  in inter-subject mode.

#### B. Angle Models

Table II summarizes the results obtained with the different models, among which W6 is the best performing.

#### C. Moment Models

For the ankle-only model, the intra-subject method achieved an  $\text{NRMSE} \pm 0.83\%$  with a correlation coefficient of  $0.97 \pm 0.01$ , while the inter-subject method resulted in an  $\text{NRMSE} \pm 1.60\%$  with a correlation coefficient of  $0.93 \pm 0.03$ .

Extending to the 5-joint models, the intra-subject method achieved a minimum  $\text{NRMSE} \pm 0.03\%$  for hip rotation moment prediction and a maximum  $\text{NRMSE} \pm 0.03\%$  for hip adduction; the lowest correlation coefficient of  $0.97 \pm 0.00$  was obtained for hip adduction, whereas the knee joint had the best correlation coefficient of  $0.9952 \pm 0.00$ . As for the inter-subject method, a minimum  $\text{NRMSE} \pm 0.64\%$  for hip flexion moment prediction and a maximum  $\text{NRMSE} \pm 1.70\%$  for the ankle joint were obtained, along with a minimum correlation coefficient of  $0.98 \pm 0.00$  for the joint, and a maximum correlation coefficient of  $0.90 \pm 0.01$  for the joint. The full results are shown in Table III.

#### D. Real-Time System

The GRF, angle, and moment predictor blocks finish 5, 14, and 23 ms after the end of the 20s data collection window. Figs. 2–4 show the real time predictions versus the average curves obtained during the initial offline data collection across all subjects, along with the standard deviation of the initial data and offline predictions (from testing in sections 3.1 to 3.3) combined. Table IV shows the  $r$  and  $r^2$  values for all prediction stages.

### IV. DISCUSSION

#### A. GRF Model

In this work, we standardized the FSR sensor data and applied weight normalization to GRF, as FSRs are unable to measure kinetic parameters, i.e. weight-induced changes in GRF, but are capable of capturing the relative distribution of plantar pressure. Hence, the values predicted by the network have to be scaled by the subject's weight to yield the true GRF [31].

Machine learning techniques are often used to estimate GRF from insole data. Oubre *et al.* [31] used the Random Forest algorithm to predict triaxial GRF and obtained a total  $\text{NRMSE}$  of 4.9% and a per-subject  $\text{NRMSE}$  of 7.7% (BW) for the

TABLE II  
SUMMARY TABLE COMPILING THE RMSE RESULTS FROM ALL THE ANGLE MODELS

Model (I/O)	Mode	Hip Flexion	Hip Adduction	Hip Rotation	Knee Flexion	Ankle Flexion
W1 (20/1)	Intra					$5.45 \pm 0.22^\circ$
	Inter					$9.06 \pm 1.80^\circ$
W2 (21/1)	Intra					$5.11 \pm 0.18^\circ$
	Inter					$9.08 \pm 2.14^\circ$
W3 (40/2)	Intra					$4.41 \pm 0.56^\circ$
	Inter					$8.71 \pm 2.21^\circ$
W4 (20/5)	Intra	$6.40 \pm 0.91^\circ$	$3.23 \pm 0.12^\circ$	$5.30 \pm 0.25^\circ$	$7.48 \pm 1.21^\circ$	$5.45 \pm 0.30^\circ$
	Inter	$9.14 \pm 2.96^\circ$	$4.81 \pm 0.96^\circ$	$7.03 \pm 1.76^\circ$	$11.00 \pm 3.69^\circ$	$9.06 \pm 2.06^\circ$
W5 (21/5)	Intra	$5.61 \pm 0.38^\circ$	$3.15 \pm 0.10^\circ$	$5.21 \pm 0.12^\circ$	$6.09 \pm 0.88^\circ$	$5.08 \pm 0.18^\circ$
	Inter	$7.48 \pm 1.53^\circ$	$4.69 \pm 0.99^\circ$	$7.32 \pm 1.60^\circ$	$9.39 \pm 2.46^\circ$	$8.66 \pm 2.04^\circ$
W6 (40/10)	Intra	$4.80 \pm 0.70^\circ$	$2.60 \pm 0.14^\circ$	$4.57 \pm 0.38^\circ$	$5.19 \pm 1.56^\circ$	$4.16 \pm 0.59^\circ$
	Inter	$8.15 \pm 1.84^\circ$	$4.97 \pm 1.15^\circ$	$7.67 \pm 2.16^\circ$	$10.07 \pm 3.08^\circ$	$8.39 \pm 2.44^\circ$

TABLE III  
EVALUATION METRICS OF THE DEEP LEARNING MODELS IN INTRA- AND INTER-SUBJECT MODES

Method	Joint	NRMSE (%)	NMAE (%)	$R^2$	$r$
Intra-subject	Hip Flexion	$2.48 \pm 0.06$	$1.85 \pm 0.03$	$0.98 \pm 0.00$	$0.99 \pm 0.00$
	Hip Adduction	$2.96 \pm 0.03$	$2.27 \pm 0.01$	$0.94 \pm 0.00$	$0.97 \pm 0.00$
	Hip Rotation	$1.63 \pm 0.03$	$1.20 \pm 0.02$	$0.98 \pm 0.00$	$0.99 \pm 0.00$
	Knee Flexion	$1.87 \pm 0.12$	$1.04 \pm 0.03$	$0.99 \pm 0.00$	$1.00 \pm 0.00$
	Ankle Flexion	$1.68 \pm 0.08$	$1.22 \pm 0.05$	$0.98 \pm 0.00$	$0.99 \pm 0.00$
Inter-subject	Hip Flexion	$6.59 \pm 0.64$	$4.85 \pm 0.55$	$0.78 \pm 0.04$	$0.90 \pm 0.01$
	Hip Adduction	$9.90 \pm 0.65$	$6.87 \pm 0.49$	$0.75 \pm 0.05$	$0.87 \pm 0.03$
	Hip Rotation	$8.23 \pm 1.35$	$6.11 \pm 1.07$	$0.67 \pm 0.08$	$0.84 \pm 0.04$
	Knee Flexion	$8.17 \pm 1.29$	$5.82 \pm 0.86$	$0.67 \pm 0.10$	$0.87 \pm 0.04$
	Ankle Flexion	$10.50 \pm 1.70$	$5.57 \pm 1.38$	$0.74 \pm 0.08$	$0.88 \pm 0.03$

vertical component, with an  $r^2$  of 0.91. Zhang *et al.* [29] used a deep dual-stream cross attention model to estimate triaxial GRF, and obtained an NRMSE of 4.16% (BW) without using cross validation or leaving subjects out. Hajizadeh *et al.* [30] estimated 3D GRF using LSTM networks, resulting in an NRMSE of 5.5% (BW). Choi *et al.* [32] used 3 different network architectures for GRF prediction, based on Artificial Neural Networks (ANN), CNN, and a combination of CNN and Long Short-Term Memory (LSTM) networks; however, they did not apply body weight normalization to the input data and reported the RMSE in N which makes it difficult to compare results. Assuming GRF can reach up to 1.2 times body weight [42], with the heaviest subject having a mass of 79 kg, their best NRMSE can therefore be approximated to 16.77%. Hence, our models achieve comparable results to the literature.

### B. Angle Models

Our purpose was to estimate lower limb joint angles based on data from 9-axis IMUs placed on the shanks and feet using machine learning based on the Random Forest algorithm. Looking at the summary Table II, among the ankle-only models, the lowest RMSEs of  $4.41 \pm 0.56^\circ$  and  $8.71 \pm 2.21^\circ$  in intra- and inter-subject modes, respectively, were obtained with the bilateral 4 IMUs + 2 vGRF model (W3). Expanding the 5-joint models, the same trend holds, as W6 performs the best ( $4.16 \pm 0.59^\circ$  and  $8.39 \pm 2.44^\circ$ ). W5 performs better than W4, and despite W2 having a similar performance to W1 in inter-subject mode (harder generalization which can be attributed mostly to inter-subject variability over more input variables), it

performs better in intra-subject mode, which reflects the benefit of adding vGRF to the feature set on the quality of the predictions. The expansion to bilateral models seems beneficial, as W3 and W6 perform better than W2 and W5, respectively, and S2 best ( $5.79 \pm 0.17^\circ$  and  $11.20 \pm 4.01^\circ$ ) performs better than S1. The addition of GRF and bilateral expansion in intra-subject mode gradually improved the performance of ankle-only models (W3 better than W2 better than W1) in the same way as the 5-joint models (W6 better than W5 better than W4), which seems logical as adding more relevant features provides more contextual information and normally improves the performance of machine learning models.

When expanding to the 5-output model, it is interesting how IMUs placed on the shanks and feet can contribute to the prediction of not only neighboring distal ankle and knee angles, but also proximal 3D hip angles, showing that all joint angles are closely related, which was taken by [28] as far as predicting hip, knee, and ankle angles with only one IMU placed on the shank.

While lower-limb joint angles have been obtained from IMUs without using machine learning, such as in [43], [44], or using different inputs such as surface EMG [45], machine learning has been frequently used to predict angles from IMU data. Ackland *et al.* [23] used accelerometer and gyroscope data from IMUs placed on the pelvis, thighs, shanks, and feet to estimate 3D angles at hip, knee, and ankle with a generative adversarial network (GAN), resulting in an RMSE of  $1.8 - 5.3^\circ$  for ankle flexion, down to  $0.6^\circ$  for hip rotation ( $0.1^\circ$  for knee abduction) and up to  $7.3^\circ$  for knee flexion. Similarly,

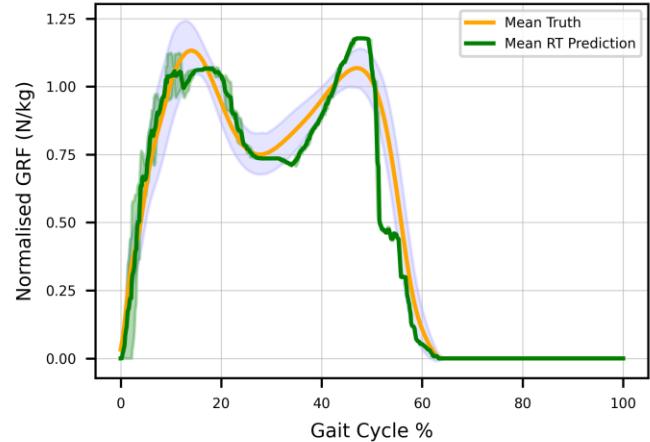
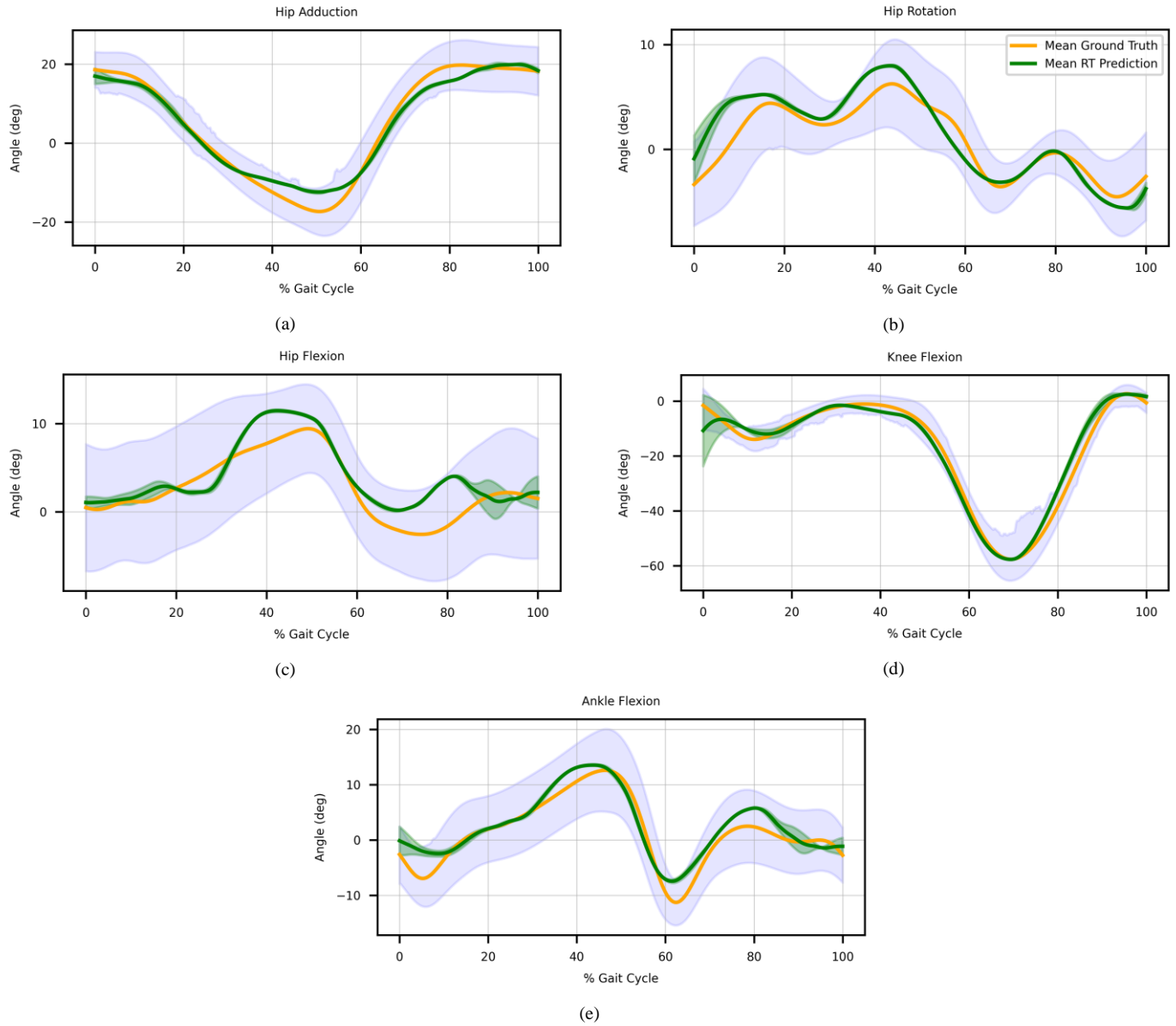


Fig. 2. Real-Time GRF versus initial ground truth data and offline predictions.

Model Name	Motion	$r$	$r^2$
GRF		0.98	0.96
	Hip Adduction	0.99	0.97
	Hip Rotation	0.93	0.73
Angles	Hip Flexion	0.88	0.62
	Knee Flexion	0.99	0.98
	Ankle Flexion	0.96	0.87
	Hip Adduction	0.94	0.79
	Hip Rotation	0.96	0.91
	Hip Flexion	0.94	0.85
Moments	Knee Flexion	0.86	0.62
	Ankle Flexion	0.96	0.92



**Fig. 3.** Ensemble averages of the real-time filtered joint angles (green) vs initial dataset (orange). The green shading represents the standard deviation of the real-time filtered data. The blue shading corresponds to the standard deviation of the initial data and the offline predictions combined.

Senanayake *et al.* [2] deployed a GAN on accelerometer and gyroscope data from IMUs placed on the thighs, shanks, and feet to predict 3D ankle angles, achieving an RMSE of  $3.6 - 5.9^\circ$  for ankle flexion (down to  $1.7^\circ$  for ankle inversion). Hollinger *et al.* [26] also used accelerometer and gyroscope data from IMUs placed on the torso, thighs, shanks, and feet, but with Random Forests to predict hip, knee, and ankle flexion angles during isolated joint movements. They obtained an RMSE of  $5.35 \pm 4.28^\circ$  for the ankle with 2 IMUs and  $5.55 \pm 4.10^\circ$  with 4 IMUs, while the knee RMSE reached  $20.71 \pm 12.41^\circ$  with 4 IMUs. Hur *et al.* [27] used data from 9-axis IMUs placed at the torso, pelvis, thighs, shanks, and feet to predict hip, knee, and ankle flexion angles with convolutional neural network (CNN) and long-short term memory (LSTM) architectures, achieving an RMSE of  $2.45 - 7.98^\circ$  at the ankle with 2 IMUs (shank and foot), up to  $8.3^\circ$  with different IMU

combinations/training methods, and up to  $17.06^\circ$  for knee angles. On the other hand, Sung *et al.* [28] used only 1 IMU placed on the shank to predict ankle, knee, and hip flexion angles using an LSTM network, achieving an RMSE of  $0.42 - 5.15^\circ$  at the ankle with an  $r^2$  of  $0.62 - 0.96$ , and up to an RMSE of  $8.14^\circ$  at the knee. Therefore, this work achieves comparable results to the literature, while predicting relatively multiple lower limb angles with a simple low latency algorithm suitable for real-time implementation.

### C. Moment Models

Our goal was to estimate ankle moments based on ankle angles and GRF using machine learning techniques. A time-series model based on the ResNet-16 architecture is introduced, achieving NRMSEs as low as 4.88%. The model was then expanded to the prediction of 5 lower limb moments

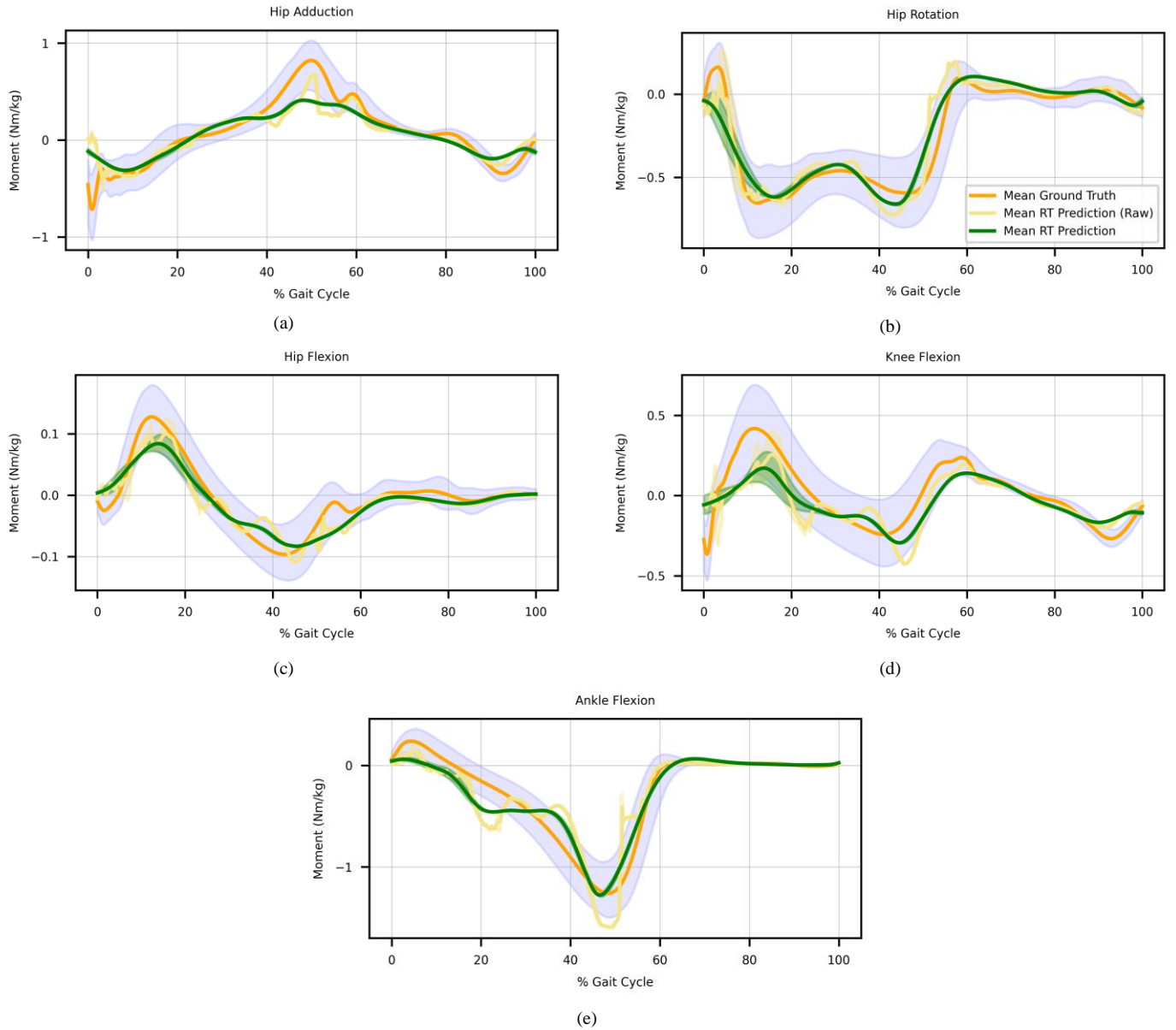


**Fig. 4.** Ensemble averages of the real-time unfiltered (purple) and filtered (green) joint moments vs initial dataset (orange).

– hip flexion, adduction, and rotation, knee flexion, and ankle flexion – using the corresponding joint angles and GRF as inputs for a similar ResNet-16 model, achieving even lower NRMSEs in the range of 1.63 – 2.96%. An expected drop in performance occurs when evaluating the model on unseen subjects in inter-subject mode, but the results remain acceptable (Table III), proving the robustness of our model.

While completely different inputs have been used for joint moment prediction in the literature, such as IMUs [46], a combination of electromyography (EMG), IMUs, and electrogoniometers [47] or EMG and muscle synergies [48], joint angles and GRF were used as well. Perrone *et al.* [49] estimated hip moments from knee flexion angles and GRF using a Long-Short Term Memory (LSTM) architecture, yielding an NRMSE of 9.62% and 15.55% NMAE. Giarmatzis *et al.* [50] predicted 3D medial and lateral knee contact forces from 13 angles spanning the human body and 3D GRF using Artificial Neural Networks (ANN) and Support Vector

Regression (SVR), achieving an NRMSE of 0.67 – 5.39%. Ozates *et al.* [41] expanded to 15 angles as inputs, and estimated ankle (flexion), knee (flexion), and hip (abduction and flexion) moments with 1D CNNs, yielding an  $8.58 \pm 3.87\%$  at the ankle in healthy subjects, compared to  $14.78 \pm 7.17\%$  in participants with cerebral palsy, up to  $12.55 \pm 5.08\%$  and  $18.02 \pm 9.14\%$ , respectively, at the knee. Mundt *et al.* [19] had slightly different settings, this time predicting 3D GRF along with 3D moments, given ankle, knee, and hip joint angles, using Feed-Forward (FF) neural networks and LSTM, and obtained an NRMSE of 8.69 – 15%. Other studies also estimated joint moments but using slightly different input combinations. For example, Xiong *et al.* [13] used 5 joint angles (3D hip, knee flexion, ankle flexion) and 10 EMG channels to predict 4 joint moments (2D hip, knee flexion, ankle flexion) with an ANN, resulting in an NRMSE of 6.70% at the ankle and 7.89% at the hip. Ardestani *et al.* [51], on the other hand, combined 2D GRF with 8 EMG channels to predict 3D hip, knee flexion, and 2D

ankle angles using an FF ANN and Wavelet Neural Networks (WNN), resulting in ankle flexion NRMSE in the range of 5 – 12%, and up to < 16% for hip adduction. Therefore, in comparison, our models achieve remarkable results with a minimal number of inputs.

#### D. Real-Time System

The objective was to achieve near real-time lower-limb motion capture, including joint angles, moments, and GRF, aiming to substitute gold-standard devices and musculoskeletal processing with a few wearable sensors and machine learning algorithms. This target was reached as the new method executes swiftly and achieves very high correlation (Pearson's  $r \geq 0.88$ ) with the expected values (Table IV), and acceptable  $r^2$  values ( $\geq 0.79$ ), except for hip rotation (0.73) and flexion (0.62) angles which tend to be relatively overestimated and knee flexion moment (0.62) which is rather underestimated, by reference to Figs. 3 and 4, but remaining mostly within one standard deviation.

Previous related work includes [52] which determines the full 3D skeletal pose in joint angles using a single RGB camera and an algorithm combining CNN and fully-connected NN, achieving a  $> 30$  fps speed with a 32.5 ms delay, [53] which estimates 3D pose using 4 cameras and up to 17 IMUs at 40 fps and overall latency of 230 ms, using a solver that optimizes the pose cost function, and [54] which determines the 3d full-body pose using acceleration and rotation data from 3 IMUs along with a combination of transformer encoder, bidirectional LSTM and multilayer perceptrons, at 60 fps with a 166ms delay. These three studies focused on full body pose, and while [52] predicted joint angles specifically, [53] adopted 3D angle-axis vectors (i.e. the axis of rotation multiplied by the angle of rotation in radians), and [54] predicted the global rotation of the pelvis and the local rotation of other joints relative to the parent joints, represented by 6-D rotation. While [52] and [53] used cameras, [55] and [56] still used standard motion capture devices, but focused on achieving a real-time data processing. [55] combined a Kalman filter, a multibody formulation, and an optimization algorithm to estimate skeletal kinematics (position, velocity, and acceleration), joint torques, and muscle efforts, respectively, with a 10 ms delay (0.8 ms inference time), and [56] which managed to use OpenSim in real time, achieving up to 2,000 fps with 31.5 ms delay. Closer to our work and [54], i.e. using wearable sensors only, [57] predicted knee angles and hip moments with an inference time of around 3 ms, using two soft stretchable capacitive sensors integrated into a knee pad. Other studies claim to have achieved real-time estimation of joint angles or moments but without providing sufficient information on the real-time implementation itself (e.g. hardware and setup) and latency, such as [50] which predicts knee moments by fusing optical motion capture and musculoskeletal modelling-derived kinematic and force variables, and [2], [23] which estimate three lower-limb joint angles using up to 3 IMUs.

Therefore, the present work stands out by (1) fully relying on wearable sensors without requiring any cameras or gold-standard motion capture systems, (2) providing estimations at 1000 fps with 23 ms delay per 20 s worth of input data, (3)

covering all five major lower limb joints, and (4) providing multimodal comprehensive estimations of GRF, joint angles, and moments. Limitations, however, include the limited size of the dataset used for training, covering only lower-limb joints, with applications restricted to walking, i.e. the movement on which the models were trained [55].

#### V. CONCLUSION

In this article, we presented a real-time, multimodal, high sample rate lower-limb motion capture framework, based on wireless wearable sensors and machine learning algorithms. The developed models achieve good accuracy compared to literature, providing predictions at 1 kHz with a minimal delay of 23 ms for 20s worth of input data. Future work can consider developing separate predictors by movement type and combining them with a motion classifier that picks the model suitable for the current detected activity. Moreover, another possible application is similar to [57], in the control of a lower-limb exoskeleton; however, the present models will need to be validated and possibly retrained for the assisted scenario as kinematic/kinetic changes can be introduced by the exoskeleton.

#### REFERENCES

- [1] H. G. Chambers and D. H. Sutherland, ‘A Practical Guide to Gait Analysis’, *JAAOS - J. Am. Acad. Orthop. Surg.*, vol. 10, no. 3, 2002, [Online]. Available: [https://journals.lww.com/jaaos/fulltext/2002/05000/a\\_practical\\_guide\\_to\\_gait\\_analysis.9.aspx](https://journals.lww.com/jaaos/fulltext/2002/05000/a_practical_guide_to_gait_analysis.9.aspx)
- [2] D. Senanayake, S. Halgamuge, and D. C. Ackland, ‘Real-time conversion of inertial measurement unit data to ankle joint angles using deep neural networks’, *J. Biomech.*, vol. 125, p. 110552, Aug. 2021, doi: 10.1016/j.jbiomech.2021.110552.
- [3] H. -S. Park, Q. Peng, and L. -Q. Zhang, ‘A Portable Telerehabilitation System for Remote Evaluations of Impaired Elbows in Neurological Disorders’, *IEEE Trans. Neural Syst. Rehabil. Eng.*, vol. 16, no. 3, pp. 245–254, June 2008, doi: 10.1109/TNSRE.2008.920067.
- [4] M. Pfeiffer and A. Hohmann, ‘Applications of neural networks in training science’, *Spec. Issue Netw. Approaches Complex Environ.*, vol. 31, no. 2, pp. 344–359, Apr. 2012, doi: 10.1016/j.humov.2010.11.004.
- [5] S. Zhang, S. Guo, B. Gao, H. Hirata, and H. Ishihara, ‘Design of a Novel Telerehabilitation System with a Force-Sensing Mechanism’, *Sensors*, vol. 15, no. 5, pp. 11511–11527, 2015, doi: 10.3390/s150511511.
- [6] A. Schmidt, ‘Movement pattern recognition in basketball free-throw shooting’, *Spec. Issue Netw. Approaches Complex Environ.*, vol. 31, no. 2, pp. 360–382, Apr. 2012, doi: 10.1016/j.humov.2011.01.003.
- [7] S. R. Iyer and R. Sharda, ‘Prediction of athletes performance using neural networks: An application in cricket team selection’, *Expert Syst. Appl.*, vol. 36, no. 3, Part 1, pp. 5510–5522, Apr. 2009, doi: 10.1016/j.eswa.2008.06.088.
- [8] M. J. Rupérez, J. D. Martín-Guerrero, C. Monserrat, and M. Alcañiz, ‘Artificial neural networks for predicting dorsal pressures on the foot surface while walking’, *Expert Syst. Appl.*,

vol. 39, no. 5, pp. 5349–5357, Apr. 2012, doi: 10.1016/j.eswa.2011.11.050.

[9] D. Joshi, A. Mishra, and S. Anand, ‘ANFIS based knee angle prediction: An approach to design speed adaptive contra lateral controlled AK prosthesis’, *Appl. Soft Comput.*, vol. 11, no. 8, pp. 4757–4765, Dec. 2011, doi: 10.1016/j.asoc.2011.07.007.

[10] R. Souron *et al.*, ‘Sex differences in active tibialis anterior stiffness evaluated using supersonic shear imaging’, *J. Biomech.*, vol. 49, no. 14, pp. 3534–3537, Oct. 2016, doi: 10.1016/j.jbiomech.2016.08.008.

[11] H. Zhang, S. Ahmad, and G. Liu, ‘Torque Estimation for Robotic Joint With Harmonic Drive Transmission Based on Position Measurements’, *Trans Rob*, vol. 31, no. 2, pp. 322–330, Apr. 2015, doi: 10.1109/TRO.2015.2402511.

[12] A. D. Prete and N. Mansard, ‘Robustness to Joint-Torque-Tracking Errors in Task-Space Inverse Dynamics’, *Trans Rob*, vol. 32, no. 5, pp. 1091–1105, Oct. 2016, doi: 10.1109/TRO.2016.2593027.

[13] B. Xiong *et al.*, ‘Intelligent Prediction of Human Lower Extremity Joint Moment: An Artificial Neural Network Approach’, *IEEE Access*, vol. 7, pp. 29973–29980, 2019, doi: 10.1109/ACCESS.2019.2900591.

[14] A. Seth, M. Sherman, J. A. Reinbolt, and S. L. Delp, ‘OpenSim: a musculoskeletal modeling and simulation framework for in silico investigations and exchange’, *Procedia IUTAM*, vol. 2, pp. 212–232, 2011, doi: <https://doi.org/10.1016/j.piutam.2011.04.021>.

[15] ‘AnyBody Technology’. [Online]. Available: [www.anybodytech.com](http://www.anybodytech.com)

[16] S. E. Oh, A. Choi, and J. H. Mun, ‘Prediction of ground reaction forces during gait based on kinematics and a neural network model’, *J. Biomech.*, vol. 46, no. 14, pp. 2372–2380, Sept. 2013, doi: 10.1016/j.jbiomech.2013.07.036.

[17] G. Leporace, L. A. Batista, L. Metsavaht, and J. Nadal, ‘Residual analysis of ground reaction forces simulation during gait using neural networks with different configurations’, presented at the Proceedings of the Annual International Conference of the IEEE Engineering in Medicine and Biology Society, EMBS, 2015, pp. 2812–2815. doi: 10.1109/EMBC.2015.7318976.

[18] W. R. Johnson, A. Mian, C. J. Donnelly, D. Lloyd, and J. Alderson, ‘Predicting athlete ground reaction forces and moments from motion capture’, *Med. Biol. Eng. Comput.*, vol. 56, no. 10, pp. 1781–1792, Oct. 2018, doi: 10.1007/s11517-018-1802-7.

[19] M. Mundt, A. Koeppe, S. David, F. Bamer, W. Potthast, and B. Markert, ‘Prediction of ground reaction force and joint moments based on optical motion capture data during gait’, *Med. Eng. Phys.*, vol. 86, pp. 29–34, Dec. 2020, doi: 10.1016/j.medengphy.2020.10.001.

[20] W. W. T. Lam, Y. M. Tang, and K. N. K. Fong, ‘A systematic review of the applications of markerless motion capture (MMC) technology for clinical measurement in rehabilitation’, *J. NeuroEngineering Rehabil.*, vol. 20, no. 1, p. 57, May 2023, doi: 10.1186/s12984-023-01186-9.

[21] K. Das, T. de Paula Oliveira, and J. Newell, ‘Comparison of markerless and marker-based motion capture systems using 95% functional limits of agreement in a linear mixed-effects modelling framework’, *Sci. Rep.*, vol. 13, no. 1, p. 22880, Dec. 2023, doi: 10.1038/s41598-023-49360-2.

[22] P. Sheahan, ‘Budgeting for a Markerless System’. [Online]. Available: <https://www.theiamarkerless.com/blog/budgeting-for-a-markerless-system>

[23] D. C. Ackland, Z. Fang, and D. Senanayake, ‘A machine learning approach to real-time calculation of joint angles during walking and running using self-placed inertial measurement units’, *Gait Posture*, vol. 118, pp. 85–91, May 2025, doi: 10.1016/j.gaitpost.2025.01.028.

[24] Z. Fang, S. Woodford, D. Senanayake, and D. Ackland, ‘Conversion of Upper-Limb Inertial Measurement Unit Data to Joint Angles: A Systematic Review’, *Sensors*, vol. 23, no. 14, 2023, doi: 10.3390/s23146535.

[25] J. C. van den Noort, S. H. Wiertsema, K. M. C. Hekman, C. P. Schönhuth, J. Dekker, and J. Harlaar, ‘Measurement of scapular dyskinesis using wireless inertial and magnetic sensors: Importance of scapula calibration’, *J. Biomech.*, vol. 48, no. 12, pp. 3460–3468, Sept. 2015, doi: 10.1016/j.jbiomech.2015.05.036.

[26] D. Hollinger, M. C. Schall, H. Chen, and M. Zabala, ‘The Effect of Sensor Feature Inputs on Joint Angle Prediction across Simple Movements’, *Sensors*, vol. 24, no. 11, 2024, doi: 10.3390/s24113657.

[27] B. Hur, S. Baek, I. Kang, and D. Kim, ‘Learning based lower limb joint kinematic estimation using open source IMU data’, *Sci. Rep.*, vol. 15, no. 1, p. 5287, Feb. 2025, doi: 10.1038/s41598-025-89716-4.

[28] J. Sung *et al.*, ‘Prediction of Lower Extremity Multi-Joint Angles during Overground Walking by Using a Single IMU with a Low Frequency Based on an LSTM Recurrent Neural Network’, *Sensors*, vol. 22, no. 1, 2022, doi: 10.3390/s22010053.

[29] D. Zhang, Y. Liu, T. Exell, Y. Huang, D. Zhou, and L. Guo, ‘Estimation of three-dimensional ground reaction forces using low-cost smart insoles’, *Intell. Sports Health*, vol. 1, no. 1, pp. 40–50, Jan. 2025, doi: <https://doi.org/10.1016/j.ish.2024.12.005>.

[30] M. Hajizadeh, A. L. Clouthier, M. Kendall, and R. B. Graham, ‘Predicting vertical and shear ground reaction forces during walking and jogging using wearable plantar pressure insoles’, *Gait Posture*, vol. 104, pp. 90–96, July 2023, doi: <https://doi.org/10.1016/j.gaitpost.2023.06.006>.

[31] B. Oubre, S. Lane, S. Holmes, K. Boyer, and S. I. Lee, ‘Estimating Ground Reaction Force and Center of Pressure Using Low-Cost Wearable Devices’, *IEEE Trans. Biomed. Eng.*, vol. 69, no. 4, pp. 1461–1468, 2022, doi: 10.1109/TBME.2021.3120346.

[32] H. S. Choi, S. Yoon, J. Kim, H. Seo, and J. K. Choi, ‘Calibrating Low-Cost Smart Insole Sensors with Recurrent Neural Networks for Accurate Prediction of Center of Pressure’, *Sensors*, vol. 24, no. 15, p. 4765, 2024.

[33] M. Porta, S. Kim, M. Pau, and M. A. Nussbaum, ‘Classifying diverse manual material handling tasks using a single wearable sensor’, *Appl. Ergon.*, vol. 93, p. 103386, May 2021, doi: 10.1016/j.apergo.2021.103386.

[34] K. Kim and Y. K. Cho, ‘Effective inertial sensor quantity and locations on a body for deep learning-based worker’s

motion recognition', *Autom. Constr.*, vol. 113, p. 103126, May 2020, doi: 10.1016/j.autcon.2020.103126.

[35] H. Zhao *et al.*, 'Prediction of Joint Angles Based on Human Lower Limb Surface Electromyography', *Sensors*, vol. 23, no. 12, 2023, doi: 10.3390/s23125404.

[36] F. Hutter, L. Xu, H. H. Hoos, and K. Leyton-Brown, 'Algorithm runtime prediction: Methods & evaluation', *Artif. Intell.*, vol. 206, pp. 79–111, Jan. 2014, doi: 10.1016/j.artint.2013.10.003.

[37] W. Dong, C. Liu, Q. Zhang, and C. Xiong, 'Design and Evaluation of an Active Ankle Exoskeleton in Gait Assistance', presented at the 2019 IEEE/ASME International Conference on Advanced Intelligent Mechatronics (AIM), July 2019, pp. 318–322. doi: 10.1109/AIM.2019.8868740.

[38] M. Lee *et al.*, 'A Compact Ankle Exoskeleton With a Multiaxis Parallel Linkage Mechanism', *IEEE/ASME Trans. Mechatron.*, vol. 26, no. 1, pp. 191–202, 2021, doi: 10.1109/TMECH.2020.3008372.

[39] C. Tang, W. Yi, J. M. Kim, and L. G. Occhipinti, 'EMG-Based Human Motion Analysis: A Novel Approach Using Towel Electrodes and Transfer Learning', presented at the 2023 IEEE SENSORS, Nov. 2023, pp. 1–4. doi: 10.1109/SENSORS556945.2023.10325287.

[40] S. Ruhrberg Estévez, J. Mallah, D. Kazieczko, C. Tang, and L. G. Occhipinti, 'Deep learning for motion classification in ankle exoskeletons using surface EMG and IMU signals', *Sci. Rep.*, vol. 15, no. 1, p. 38242, Oct. 2025, doi: 10.1038/s41598-025-22103-1.

[41] M. E. Ozates, D. Karabulut, F. Salami, S. I. Wolf, and Y. Z. Arslan, 'Machine learning-based prediction of joint moments based on kinematics in patients with cerebral palsy', *J. Biomech.*, vol. 155, p. 111668, June 2023, doi: 10.1016/j.jbiomech.2023.111668.

[42] J. Blaya, 'Force-controllable ankle foot orthosis (AFO) to assist drop foot gait', 26 2005.

[43] S. Zihajehzadeh, P. K. Yoon, B. -S. Kang, and E. J. Park, 'UWB-Aided Inertial Motion Capture for Lower Body 3-D Dynamic Activity and Trajectory Tracking', *IEEE Trans. Instrum. Meas.*, vol. 64, no. 12, pp. 3577–3587, Dec. 2015, doi: 10.1109/TIM.2015.2459532.

[44] C. Yi, B. Wei, Z. Ding, C. Yang, Z. Chen, and F. Jiang, 'A Self-Aligned Method of IMU-Based 3-DoF Lower-Limb Joint Angle Estimation', *IEEE Trans. Instrum. Meas.*, vol. 71, pp. 1–10, 2022, doi: 10.1109/TIM.2022.3194935.

[45] K. Zhang, S. Wen, Z. An, C. Wang, F. Wang, and Q. Ding, 'PT-ATN: Cross-Subject Lower Limb Joint Angle Estimation Under Small-Sample Data', *IEEE Trans. Instrum. Meas.*, vol. 74, pp. 1–11, 2025, doi: 10.1109/TIM.2025.3625613.

[46] M. Mundt *et al.*, 'Estimation of Gait Mechanics Based on Simulated and Measured IMU Data Using an Artificial Neural Network', *Front. Bioeng. Biotechnol.*, vol. Volume 8-2020, 2020, doi: 10.3389/fbioe.2020.00041.

[47] J. Camargo, D. Molinaro, and A. Young, 'Predicting biological joint moment during multiple ambulation tasks', *J. Biomech.*, vol. 134, p. 111020, Mar. 2022, doi: 10.1016/j.jbiomech.2022.111020.

[48] Y. -X. Liu and E. M. Gutierrez-Farewik, 'Muscle synergies enable accurate joint moment prediction using few electromyography sensors', in *2021 IEEE/RSJ International Conference on Intelligent Robots and Systems (IROS)*, Oct. 2021, pp. 5090–5097. doi: 10.1109/IROS51168.2021.9636696.

[49] M. Perrone, S. P. Mell, J. Martin, S. J. Nho, and P. Malloy, 'Machine learning-based prediction of hip joint moment in healthy subjects, patients and post-operative subjects', *Comput. Methods Biomed. Engin.*, pp. 1–5, doi: 10.1080/10255842.2024.2310732.

[50] G. Giarmatzis, E. I. Zacharaki, and K. Moustakas, 'Real-Time Prediction of Joint Forces by Motion Capture and Machine Learning', *Sensors*, vol. 20, no. 23, 2020, doi: 10.3390/s20236933.

[51] M. M. Ardestani *et al.*, 'Human lower extremity joint moment prediction: A wavelet neural network approach', *Expert Syst. Appl.*, vol. 41, no. 9, pp. 4422–4433, July 2014, doi: 10.1016/j.eswa.2013.11.003.

[52] D. Mehta *et al.*, 'XNect: real-time multi-person 3D motion capture with a single RGB camera', *ACM Trans Graph*, vol. 39, no. 4, Aug. 2020, doi: 10.1145/3386569.3392410.

[53] C. Malleson, J. Collomosse, and A. Hilton, 'Real-Time Multi-person Motion Capture from Multi-view Video and IMUs', *Int. J. Comput. Vis.*, vol. 128, no. 6, pp. 1594–1611, June 2020, doi: 10.1007/s11263-019-01270-5.

[54] Z. Zhu *et al.*, 'Progressive Inertial Poser: Progressive Real-Time Kinematic Chain Estimation for 3-D Full-Body Pose From Three IMU Sensors', *IEEE Trans. Instrum. Meas.*, vol. 74, pp. 1–13, 2025, doi: 10.1109/TIM.2025.3570339.

[55] U. Lugrís, M. Pérez-Soto, F. Michaud, and J. Cuadrado, 'Human motion capture, reconstruction, and musculoskeletal analysis in real time', *Multibody Syst. Dyn.*, vol. 60, no. 1, pp. 3–25, Jan. 2024, doi: 10.1007/s11044-023-09938-0.

[56] C. Pizzolato, M. Reggiani, L. Modenese, and D. G. Lloyd, 'Real-time inverse kinematics and inverse dynamics for lower limb applications using OpenSim', *Comput. Methods Biomed. Engin.*, vol. 20, no. 4, pp. 436–445, Mar. 2017, doi: 10.1080/10255842.2016.1240789.

[57] L. Feng *et al.*, 'Locomotion Joint Angle and Moment Estimation With Soft Wearable Sensors for Personalized Exosuit Control', *IEEE Trans. Neural Syst. Rehabil. Eng.*, vol. 33, pp. 1048–1060, 2025, doi: 10.1109/TNSRE.2025.3547361.